



# HHS Public Access

Author manuscript

*Mucosal Immunol.* Author manuscript; available in PMC 2014 January 01.

Published in final edited form as:

*Mucosal Immunol.* 2013 July ; 6(4): 847–856. doi:10.1038/mi.2012.123.

## Retinoic acid regulates the development of a gut homing precursor for intestinal dendritic cells

Ruizhu Zeng<sup>1,2</sup>, Cecilia Oderup<sup>1,2</sup>, Robert Yuan<sup>1,2</sup>, Mike Lee<sup>1,2</sup>, Aida Habtezion<sup>3</sup>, Husein Hadeiba<sup>1,2</sup>, and Eugene C Butcher<sup>1,2</sup>

<sup>1</sup>Laboratory of Immunology and Vascular Biology, Department of Pathology, Stanford University School of Medicine, Stanford, CA 94305, USA

<sup>2</sup>The Center for Molecular Biology and Medicine, Veterans Affairs Palo Alto Health Care System, Palo Alto, CA 94304, USA

<sup>3</sup>Medicine/Gastroenterology, Stanford University School of Medicine, Stanford, CA 94305, USA

### Abstract

The vitamin A metabolite retinoic acid (RA) regulates intestinal immune responses through immunomodulatory actions on intestinal dendritic cells (DCs) and lymphocytes. Here, we show that retinoic acid also controls the generation of gut-tropic migratory DC precursors, referred to as pre-mucosal DCs (pre- $\mu$ DCs). Pre- $\mu$ DCs express the gut trafficking receptor  $\alpha 4\beta 7$  and home preferentially to the intestines. They develop in the bone marrow, can differentiate into CCR9<sup>+</sup> plasmacytoid DCs as well as conventional DCs (cDCs), but preferentially give rise to CD103<sup>+</sup> intestinal cDCs. Generation of pre- $\mu$ DCs *in vivo* in the bone marrow or *in vitro* is regulated by RA and retinoic acid receptor  $\alpha$  signaling. The frequency of pre- $\mu$ DCs is reduced in vitamin A-deficient animals and in animals treated with retinoic acid receptor inhibitors. The results define a novel vitamin A-dependent, retinoic-acid-regulated developmental sequence for dendritic cells and identify a targeted precursor for CD103<sup>+</sup> cDCs in the gut.

### INTRODUCTION

The maintenance of steady-state tolerance to commensal flora and the ability to rapidly clear pathogens in case of gut wall disruption require flexibility and sophistication in the mucosal immune system. Specialized antigen-presenting dendritic cells (DCs) in the gut wall and gut-associated lymphoid tissues (GALT) control the balance between intestinal immunity and inflammation<sup>1–9</sup>. It is now clear that vitamin A and its metabolite retinoic acid (RA)

Users may view, print, copy, and download text and data-mine the content in such documents, for the purposes of academic research, subject always to the full Conditions of use:[http://www.nature.com/authors/editorial\\_policies/license.html#terms](http://www.nature.com/authors/editorial_policies/license.html#terms)

Address correspondence: Eugene C. Butcher, Department of Pathology, Stanford University School of Medicine, Stanford, CA 94305-5324, USA, tel: (650) 852-3369, fax: (650) 858-3986, [ebutcher@stanford.edu](mailto:ebutcher@stanford.edu), [ruizhu@stanford.edu](mailto:ruizhu@stanford.edu).

The authors declare no conflict of interest.

#### **AUTHOR CONTRIBUTIONS**

R.Z. designed and performed experiments and wrote the manuscript; C.O. carried out early phenotypic and other studies that led to the definition of pre- $\mu$ DC, and performed the homing studies; R.Y. and M.L. performed experiments; H.H. was involved in the initiation of the project, including initial studies of pre- $\mu$ DC development, and provided advice; A.H. assisted with the homing study and provided advice; E.C.B. directed the study and wrote the manuscript. All authors reviewed and commented on the manuscript.

play critical roles in the local differentiation and function of intestinal DCs, especially the migratory CD103<sup>+</sup> populations<sup>10</sup>. RA programs CD103<sup>+</sup> DCs to upregulate retinaldehyde dehydrogenase (RALDH), the rate-limiting enzyme for conversion of vitamin A precursors into retinoic acid<sup>10</sup>. These mucosal DCs migrate to the draining mesenteric lymph nodes where they present RA along with processed antigen to T cells<sup>2,4</sup>. RA imprints responding T cells with gut homing properties<sup>11</sup> and, in the absence of danger signals, favors the induction of tolerogenic regulatory T cells<sup>8</sup> by suppressing memory/effector T cell mediated inhibition of Treg conversion from naïve T cells<sup>12</sup>. Thus RA plays a critical local role in intestinal dendritic cell function and immune regulation, but its involvement in the origin of intestinal DC precursors has not been studied.

Here we describe a targeted gut homing DC precursor, designated pre-mucosal DCs (pre- $\mu$ DCs), whose development in the bone marrow is regulated by retinoic acid. Pre- $\mu$ DCs are identifiable phenotypically as lineage<sup>-</sup>CD11c<sup>int</sup>B220<sup>+</sup>CCR9<sup>-</sup> cells that express the intestinal homing receptor  $\alpha$ 4 $\beta$ 7. They can arise *in vitro* from CD11c<sup>int</sup>B220<sup>+</sup> bone marrow precursors that lack both CCR9 and  $\alpha$ 4 $\beta$ 7. Pre- $\mu$ DCs give rise to CCR9<sup>+</sup> plasmacytoid DCs (pDCs) and to conventional DCs (cDCs), and home preferentially to the intestines *in vivo*. They are particularly efficient at generating CD103<sup>+</sup> cDCs *in vitro* and replenishing intestinal CD103<sup>+</sup> cDCs *in vivo*. RA signaling through retinoic acid receptor  $\alpha$  (RAR $\alpha$ ) drives pre- $\mu$ DC differentiation from bone marrow progenitors, and the frequency of pre- $\mu$ DCs was reduced in vitamin A-deficient animals and in animals treated with an inhibitor of RAR signaling. Retinoic acid thus plays a unifying role in intestinal DC development and function, regulating both the generation of gut-homing precursors and the specialized functions of DC within the gut environment.

## RESULTS

### Identification of a phenotypically unique $\alpha$ 4 $\beta$ 7<sup>+</sup> DC subset *in vivo*

In studies of DC subsets expressing B220, we discovered a subset of B220<sup>+</sup>CD11c<sup>int</sup> DCs that expresses the  $\alpha$ 4 $\beta$ 7 integrin, a homing receptor that mediates lymphocyte recruitment into the intestinal wall through interaction with the mucosal vascular addressin MAdCAM1<sup>13</sup> (Figs. 1a and S1a).  $\alpha$ 4 $\beta$ 7<sup>+</sup>B220<sup>+</sup> DCs are found in secondary lymphoid tissues and the bone marrow (BM), and are particularly prominent among the B220<sup>+</sup> DCs in the gut-associated mesenteric lymph nodes (MLN) and in the small intestine (SI) lamina propria (LP) (Figs. 1a and S1a). These cells are phenotypically distinct from previously described peripheral or BM DC populations or precursors, including splenic cDCs, BM CCR9<sup>+</sup> pDCs, common DC progenitors (CDPs), and pre-cDCs (Figs. S1b and S1c). We took advantage of an Fms-like tyrosine kinase 3 ligand (Flt3L)-expressing B16 melanoma to expand DC subsets *in vivo* with minimal alterations in their phenotypic or functional capabilities for homing and adoptive transfer studies<sup>14</sup>. The  $\alpha$ 4 $\beta$ 7<sup>+</sup>B220<sup>+</sup> DCs were dramatically expanded in Flt3L-treated mice, suggesting a proliferative or progenitor potential (Fig. 1b). We refer to them hereafter as pre- $\mu$ DCs, short for pre-mucosal DCs.

We hypothesized that, by virtue of their expression of  $\alpha$ 4 $\beta$ 7, pre- $\mu$ DCs might home efficiently from the blood into the gut wall. Pre- $\mu$ DCs were sorted from lymphoid tissues of Flt3L-treated B6.CD45.2 mice. Localization *in vivo* was assessed 3 days after intravenous

transfer into congenic B6.CD45.1 recipients. Pre- $\mu$ DCs preferentially homed to the SI LP (Fig. 1c). Preferential homing of pre- $\mu$ DCs to the SI LP and colon was also apparent in shorter-term (12-hour) homing studies (data not shown).

### Pre- $\mu$ DCs give rise to CCR9<sup>+</sup> pDCs and to CD103<sup>+</sup> cDCs *in vitro*

To assess the progenitor potential of pre- $\mu$ DCs, we sorted them from BM and cultured them *in vitro* with total BM cells taken from CD45 allotype congenic mice as feeder cells (Fig. 2a). In some experiments, we also used pre- $\mu$ DCs sorted from the BM of Flt3L-treated mice; these cells are phenotypically similar to normal BM pre- $\mu$ DCs, the classical CCR9<sup>+</sup> pDC markers PDCA1, Siglec H, and Ly6c are down-regulated, not unlike the surface phenotype of pre- $\mu$ DCs in normal spleen (data not shown). Cells were cultured with recombinant Flt3L and their progeny were analyzed by flow cytometry after 3–6 days. By day 3–4, the cultures contained three prominent and phenotypically distinctive pre- $\mu$ DC-derived populations (Figs. 2b and 2c): CCR9<sup>+</sup> pDCs, which retained high levels of B220 and intermediate expression of CD11c; CD103<sup>+</sup> DCs that were  $\alpha 4\beta 7^-$  CCR9<sup>-</sup> B220<sup>-</sup> and CD11c<sup>+</sup>, essentially a cDC phenotype; and a population of  $\alpha 4\beta 7^+$  pre- $\mu$ DC-like cells whose phenotype (lower B220 and slightly higher CD11c levels than starting pre- $\mu$ DCs) appeared transitional between that of BM pre- $\mu$ DCs and cDCs. In fact, a fraction of the  $\alpha 4\beta 7^+$  DC had upregulated CD103. By day 6 pre- $\mu$ DC-derived progeny were mostly CD103<sup>+</sup> cDC (70–80%, N>3) (Fig. 2c). However, the absolute numbers of all three subsets peaked on day 3 and decreased by day 6, suggesting limited life span of pre- $\mu$ DC and their progeny *in vitro* (Fig. S2a). Similar results were seen whether pre- $\mu$ DCs were from normal or Flt3L-treated mouse BM (Figs. 2b and 2c). Consistent with prior studies of Flt3L-driven *in vitro* BM-derived cDC, pre- $\mu$ DC progeny *in vitro* did not express surface CD8 $\alpha$  (data not shown). The results demonstrate that pre- $\mu$ DCs can give rise rapidly to both classical CCR9<sup>+</sup> pDCs and to CD103<sup>+</sup> cDCs. We were unsuccessful in efforts to evaluate pre- $\mu$ DC development at the clonal level and therefore cannot exclude the possibility that distinct pDC and cDC precursors exist within the gut-tropic pre- $\mu$ DC pool.

### Pre- $\mu$ DCs give rise to CCR9<sup>+</sup> pDCs and to CD103<sup>+</sup> cDCs *in vivo*

We next assessed the development of pre- $\mu$ DC *in vivo* in a homeostatic setting. We sorted pre- $\mu$ DCs from Flt3L-treated B6.CD45.2 mice and injected them into congenic B6.CD45.1 recipients. Recipient mice were sacrificed on day 4 or 7. On day 4 after transfer, both cDCs and CCR9<sup>+</sup> pDCs were observed among CD45.2<sup>+</sup> pre- $\mu$ DC-derived progeny cells in the spleen, small intestine, and lung. In the intraepithelial lymphocytes (IEL), CCR9<sup>+</sup> pDCs (CD11c<sup>int</sup>B220<sup>+</sup>CCR9<sup>+</sup>) predominated among pre- $\mu$ DC-derived cells (Fig. 3a, left). In the SI LP, a subset of transferred cells maintained the pre- $\mu$ DC phenotype ( $\alpha 4\beta 7^+$ , CD103<sup>-</sup>), with some showing reduced B220 expression (Fig. 3a, right). Pre- $\mu$ DC progeny in the SI LP and in other tissues analyzed were mainly CD103<sup>+</sup> cDCs (mucosal tissues) or CD8 $\alpha^+$  cDC (in the spleen) on both day 4 and 7 (Fig. 3b; and data not shown). By day 7, most pre- $\mu$ DC-derived CCR9<sup>+</sup> pDCs and pre- $\mu$ DC themselves had disappeared from all tissues, suggesting rapid turnover of pre- $\mu$ DC-derived CCR9<sup>+</sup> pDCs and a limited self-renewal capacity of pre- $\mu$ DCs. Consistent with their preferential homing to the SI LP, a higher percentage of cDCs in the SI LP than in the spleen or the lung originated from pre- $\mu$ DCs (Fig. 3c). Similar results were seen in lethally irradiated recipients (Fig. S2b). Intestinal CD103<sup>+</sup> cDCs

comprise 2 distinct subsets: CD11b<sup>+</sup> and CD11b<sup>-</sup>. Pre- $\mu$ DCs gave rise to both CD103<sup>+</sup>CD11b<sup>-</sup> and CD103<sup>+</sup>CD11b<sup>+</sup> intestinal cDCs in the SI LP (Figs. 3b and d). The intestinal CD103<sup>+</sup>CD11b<sup>-</sup> cDCs are developmentally related to the splenic CD8a<sup>+</sup>CD11b<sup>-</sup> cDCs, as their development depends on common transcription factors<sup>15,16</sup>. No developmental equivalent of the intestinal CD103<sup>+</sup>CD11b<sup>+</sup> cDCs have been identified in the spleen. Most of the pre- $\mu$ DC-derived CD8a<sup>+</sup>CD11b<sup>-</sup> cDCs in the spleen expressed a low level of CD103 (data not shown). Bogunovic M. *et al* have shown that migratory pre-cDC (Lineage<sup>-</sup>CD11c<sup>+</sup>MHCII<sup>-</sup>CD135<sup>+</sup>Sirp $\alpha$ <sup>low</sup>) can also give rise to CD103<sup>+</sup> cDC in the SI LP<sup>2</sup>. When co-transferred with pre-cDC, pre- $\mu$ DC are 7–10 fold better than pre-cDC at giving rise to cDC in the SI LP on a per cell basis (Figure S2c). This is not surprising because unlike pre- $\mu$ DC, pre-cDC do not express gut-specific homing receptors and thus are not primed to repopulate the intestines (see Figure S1c).

Few pre- $\mu$ DC-derived cells were seen in the MLN 4 days after transfer but by day 7, significant fractions of CD103<sup>+</sup>CD11b<sup>-</sup> and CD103<sup>+</sup>CD11b<sup>+</sup> cDCs in the MLN were derived from pre- $\mu$ DCs (Fig. 3d). Given preferential homing of pre- $\mu$ DC to the LP rather than the MLN, pre- $\mu$ DCs likely differentiate into CD103<sup>+</sup> mucosal DCs in the gut wall and subsequently migrate to the MLN. This is consistent with the known migratory behavior of small intestine CD103<sup>+</sup> cDCs<sup>17</sup>. Importantly, pre- $\mu$ DC-derived cDCs (CD11c<sup>+</sup>MHCII<sup>+</sup>B220<sup>-</sup>CD103<sup>+</sup>CD11b<sup>+</sup> or CD11b<sup>-</sup>) in GALT displayed the characteristic aldehyde dehydrogenase (ALDH) activity of endogenous CD103<sup>+</sup> gut cDCs: ~50% of pre- $\mu$ DC-derived cDCs in the MLN stained strongly with Aldefluor<sup>TM</sup> (Fig. 3e), a fluorogenic substrate used to detect ALDHs important in the metabolism of retinal to retinoic acid<sup>18</sup>. In contrast, pre- $\mu$ DCs in the BM (data not shown) and pre- $\mu$ DC-derived splenic cDCs did not display ALDH activity (Fig. 3e). Thus, pre- $\mu$ DCs give rise to both CD11b<sup>+</sup> and CD11b<sup>-</sup> subsets of CD103<sup>+</sup> cDCs in the SI LP and acquire mucosal characteristics in response to the intestinal or GALT environment. Furthermore, antibody blockade of  $\alpha$ 4 $\beta$ 7 during pre- $\mu$ DC transfer drastically reduced the number of pre- $\mu$ DC-derived cDC in the LP, but not in the spleen or lung (Fig. 3f), consistent with an important role for  $\alpha$ 4 $\beta$ 7-mediated homing in the pre- $\mu$ DC contribution to the intestinal DC pool.

CD11c<sup>int</sup>B220<sup>+</sup> DCs were comprised of  $\alpha$ 4 $\beta$ 7<sup>+</sup> pre- $\mu$ DCs, CCR9<sup>+</sup> pDCs, and a subset of  $\alpha$ 4 $\beta$ 7<sup>-</sup>CCR9<sup>-</sup> (double negative or DN) cells (Fig. 1, Fig. S3a). The DN DCs are particularly abundant relative to pre- $\mu$ DCs in the bone marrow. When cultured *in vitro* with Flt3L, DN DCs gave rise rapidly (within 24 hours) to CCR9<sup>+</sup> pDCs and to  $\alpha$ 4 $\beta$ 7<sup>+</sup> pre- $\mu$ DCs (Fig. S3b). Although both DN DCs and pre- $\mu$ DCs gave rise to CCR9<sup>+</sup> pDCs *in vitro*, DN DCs did so more rapidly and resulted in a higher proportion of CCR9<sup>+</sup> pDCs (compare Fig. S3b and Figs. 2b and 2c). In contrast, sorted CCR9<sup>+</sup> pDCs retained their phenotype in culture, indicating that these cells were terminally differentiated (data not shown). Like pre- $\mu$ DCs, upon longer culture DN DCs developed into cDCs, including CD103<sup>+</sup> cDC, although cDC development from DN DCs was delayed relative to that from pre- $\mu$ DCs (Fig. S3c). When transferred into normal or irradiated recipients, DN DCs were slightly less efficient than pre- $\mu$ DC at generating cDCs in lymphoid tissues and did not preferentially contribute to intestinal vs. splenic cDC populations at the time points examined (day 5–7, Fig. S3d). These results suggest that pre- $\mu$ DCs arise from DN DCs in the BM, but that pre- $\mu$ DCs may

be more developmentally primed to migrate and reconstitute peripheral tissues, especially the intestinal tract, than are DN DCs.

### Intestinal pre- $\mu$ DCs display a transitional phenotype but retain progenitor activity

Pre- $\mu$ DCs are most highly represented within the GALT and SI LP of those tissues evaluated. Compared to BM pre- $\mu$ DCs, pre- $\mu$ DCs in the LP displayed higher expression of CD11c, but lower or no expression of pDC markers including B220, PDCA1, Ly6C, and Siglec H (Fig. 4a). LP pre- $\mu$ DCs also appeared more mature than their BM counterparts, with higher MHCII, CD11b,  $\alpha 4\beta 7$ , and CCR6 expression but similar CD80 and CD86 co-stimulatory molecule expression (Fig. 4a). Splenic pre- $\mu$ DCs had an intermediate phenotype (Fig. 4a). When cultured with Flt3L and total BM cells, SI LP pre- $\mu$ DCs retained the ability to generate CD103<sup>+</sup> cDCs; but they displayed little or no potential to give rise to pDCs (Fig. 4b). Furthermore, ~ 30% of LP pre- $\mu$ DC expressed proliferating cell nuclear antigen (PCNA) and transferred pre- $\mu$ DC can still be detected 4 days after transfer, suggesting that pre- $\mu$ DCs can proliferate locally in the SI LP (data not shown). We conclude that pre- $\mu$ DCs in the LP retain cDC progenitor activity, but have a transitional phenotype likely reflecting their programmed development into CD103<sup>+</sup> intestinal cDCs.

### Retinoic acid controls pre- $\mu$ DC development in the BM

We next asked whether RA regulates the development of  $\alpha 4\beta 7^+$  pre- $\mu$ DCs from BM progenitors. Addition of RA to cultures of total BM dramatically increased the frequency of pre- $\mu$ DCs among total progeny cells at the expense of CCR9<sup>+</sup> pDCs and DN DCs (Figs. 5a and 5b and data not shown). Consistent with a requirement for RA signaling through its nuclear receptor RAR $\alpha$ , pre- $\mu$ DC generation was also enhanced by the selective RAR $\alpha$  agonist AM580 (Figs. 5a and 5b, S4a). When cultured with delipidated serum, which is free of retinoids, fewer pre- $\mu$ DC were generated. When RA or AM580 was added to the culture with delipidated serum, pre- $\mu$ DC generation was enhanced (Fig. S4b). Furthermore, addition of the pan-RAR inverse agonist BMS493 or pan antagonist LE540 inhibited pre- $\mu$ DC development *in vitro* (Figs. 5a and 5b and data not shown). Like pre- $\mu$ DC found in the BM *in vivo*, pre- $\mu$ DC generated *in vitro* with or without RAR signaling are mostly CD103<sup>-</sup> (Fig S4c). To assess the involvement of proliferation in these effects, we labeled BM with CFSE prior to culture. Under control conditions or with the RAR antagonist, a significant fraction of developing CCR9<sup>+</sup> pDCs were derived from cells that had divided, but RA or the RAR $\alpha$  agonist almost completely eliminated this population of previously divided CCR9<sup>+</sup> pDCs. Given the limited self-proliferative potential of CCR9<sup>+</sup> pDCs, it is likely that RAR signaling directly inhibits CCR9<sup>+</sup> pDC development from progenitors in the BM. In contrast, RA signaling enhanced the percentage of  $\alpha 4\beta 7^+$  pre- $\mu$ DCs arising from dividing cells (Fig. 5c). Thus RA regulates the generation of pre- $\mu$ DC.

Manipulation of the RAR signaling pathway had similar effects on pre- $\mu$ DC development *in vivo*. Mice treated with RA and AM580 displayed an increase in pre- $\mu$ DC frequency in the BM, consistent with our *in vitro* observations. In contrast, treatment with BMS493 reduced the frequency of pre- $\mu$ DCs (Figs. 5d). More importantly, pre- $\mu$ DCs were also significantly reduced in the BM of mice fed a vitamin A-deficient diet compared to mice fed a control

diet (Fig. 5d). We conclude that vitamin A and its metabolite RA regulate the development of a targeted precursor for intestinal dendritic cells.

## DISCUSSION

We have identified a migratory common DC precursor that preferentially homes to the gut wall and gives rise to intestinal DCs, especially CD103<sup>+</sup> subsets. Pre- $\mu$ DCs have an immature phenotype and share phenotypic features with CCR9<sup>+</sup> pDCs, including expression of pDC markers such as PDCA1, Siglec H, Ly6C, and B220, but are distinguished from CCR9<sup>+</sup> pDCs by differential trafficking receptor expression and by their developmental potential. Pre- $\mu$ DCs express  $\alpha 4\beta 7$  but not CCR9 and proliferate and differentiate into cDCs and CCR9<sup>+</sup> pDCs *in vitro* and *in vivo*, whereas conventional CCR9<sup>+</sup> pDCs are  $\alpha 4\beta 7$ <sup>-</sup> and are terminally differentiated. Bone marrow pre- $\mu$ DCs are closely related to and can arise from CD11c<sup>int</sup>B220<sup>+</sup>CCR9<sup>-</sup> $\alpha 4\beta 7$ <sup>-</sup> DN DCs.

Development of pre- $\mu$ DCs in the bone marrow is regulated by retinoic acid. Treatment of BM cultures with RAR agonists increased and RAR antagonists decreased the frequency of pre- $\mu$ DCs. All trans-RA, a pan-RAR agonist, and AM580, an RAR $\alpha$  specific agonist, had similar effects on pre- $\mu$ DC development, suggesting that modulation of RAR signaling in the BM is primarily through RAR $\alpha$ . RAR signaling had a similar modulating effect on pre- $\mu$ DC development *in vivo*. Vitamin A deficiency, which leads to reduced circulating retinol<sup>11</sup>, reduced the number and frequency of pre- $\mu$ DCs in the BM. Similarly, systemic treatment of mice with the pan RAR inverse agonist BMS493 reduced pre- $\mu$ DC, whereas intraperitoneal administration of all trans-RA or the RAR $\alpha$  agonist AM580 increased the frequency and number of pre- $\mu$ DCs dramatically. RA regulates hematopoietic progenitor development, and modulation of RAR $\alpha$ /RXR signaling regulates hematopoietic stem cell (HSC) differentiation, proliferation, and self-renewal<sup>19–21</sup>. Furthermore, RA modulates neutrophil differentiation from myeloid progenitors under steady state conditions<sup>22</sup>. While BM pre- $\mu$ DCs lack ALDH activity (as indicated by Aldefluor assay; data not shown), subsets of BM hematopoietic cells, including HSCs, express retinaldehyde dehydrogenases<sup>21,23</sup>, providing a potential source for RA generation from retinol within the local bone marrow environment.

Earlier studies showed that retinoic acid regulates cDC function within the intestinal LP and GALT. RA induces the RALDH gene *Aldh1a2* in intestinal DCs<sup>10</sup>. RALDH allows intestinal cDCs to convert retinal to retinoic acid, creating a positive feedback loop and also allowing GALT DCs to present RA along with antigen to T cells. RA in turn induces T cell expression of the gut homing receptors  $\alpha 4\beta 7$  and CCR9. In this manner, T cells responding to gut antigens are programmed to traffic back to the intestines<sup>11</sup>. Interestingly, although RA also induces  $\alpha 4\beta 7$  expression on developing pre- $\mu$ DCs, it does not induce CCR9 expression. Indeed, expression of  $\alpha 4\beta 7$  and CCR9 is mutually exclusive among B220<sup>+</sup>CD11c<sup>int</sup> DCs, and RA actually suppresses the development of CCR9-expressing pDCs in our *in vitro* and *in vivo* models. Thus the signaling pathways that control expression of these trafficking receptors must differ in DCs and lymphocytes. BM pre- $\mu$ DCs do not display intrinsic aldehyde dehydrogenase activity, but we show that their CD103-expressing cDC progeny upregulate ALDH activity within the gut environment. Furthermore, pre- $\mu$ DC derived

splenic cDC and CD103<sup>+</sup>CD11b<sup>-</sup> intestinal cDC express CD8α *in vivo* but pre-μDC derived CD103<sup>+</sup> cDC do not express CD8α *in vitro*. This suggests that the *in vivo* tissue environments of the spleen or LP must comprise additional factors or stimuli not present in our *in vitro* culture system.

We focused primarily on cDC progeny in our analyses, even though pre-μDCs rapidly differentiated into CCR9<sup>+</sup> pDCs as well both *in vitro* and *in vivo*. Pre-μDC-derived pDCs were especially abundant relative to pre-μDC-derived cDCs in the BM and the IEL compartments of the gut wall of adoptive recipients. This distribution parallels the characteristic homeostatic representation of DC subsets in these sites, where classical CCR9<sup>+</sup> pDCs significantly outnumber cDCs (whereas cDCs predominate in most other tissues). Although pre-μDC-derived pDCs generated in the BM or other tissues can likely home to the gut after upregulation of CCR9, pre-μDCs may also be able to generate pDCs locally in the gut after entry from the blood. Importantly, in the gut, pre-μDC-derived pDCs appeared rapidly and then disappeared from the recipient IEL compartment within 5–6 days, whereas donor-derived intestinal cDCs remained readily detectable for at least 10 days after pre-μDC transfer. Overall, the tissue- and time-dependent representation of pre-μDC-derived pDCs and cDCs likely reflects multiple factors including environmental effects on pre-μDC differentiation into pDCs vs. cDCs, intrinsic and/or environment-specific differences in the survival and proliferation of progeny pDCs vs. cDCs, and a limited self-renewal potential of pre-μDCs. Another potential factor is the apparent progressive loss of pDC potential after pre-μDCs enter peripheral tissues, as evidenced by the inability of pre-μDCs from the SI LP to generate pDCs in culture.

In the BM, pre-μDCs are a minor subset of the B220<sup>+</sup>CD11c<sup>int</sup> DCs: The majority of B220<sup>+</sup> DCs are CCR9<sup>+</sup> pDCs and CCR9<sup>-</sup>α4β7<sup>-</sup> DN DCs. Importantly, DN DCs depleted of pre-μDCs gave rise to pre-μDCs in culture, and thus contain precursors for both pre-μDC and CCR9<sup>+</sup> pDC. DN DC conversion into CCR9<sup>+</sup> pDC and α4β7<sup>+</sup> pre-μDC phenotypes occurred rapidly, within 2 days, and did not require cell division (data not shown). DN DCs also gave rise to cDCs, including CD103<sup>+</sup> cDCs, in longer-term culture. These findings are consistent with the reported ability of splenic and BM CD11c<sup>int</sup>B220<sup>+</sup>CCR9<sup>-</sup> DCs to give rise to cDCs<sup>24,25</sup> (and see next paragraph). Moreover, culture of classical CD11c<sup>-</sup> CDPs with Flt3L also led to production of DN DCs and pre-μDCs, as well as to pDCs and cDCs (data not shown). In the simplest interpretation, our data suggest a linear model in which bone marrow progenitors such as the common DC progenitor (CDP) and possibly early progenitors such as the macrophage, dendritic cell progenitor (MDP) give rise to CD11c<sup>int</sup>B220<sup>+</sup> DN DCs, which in turn differentiate into pre-μDCs that rapidly exit the marrow and home to the gut to replenish intestinal DCs (Figure S5). However, given the emerging appreciation of nonlinear developmental sequences in hematopoiesis and of the malleability of progenitors in response to environmental signals<sup>25–27</sup>, we cannot exclude other pathways to pre-μDC development.

The gut homing ability of pre-μDC, their capacity to differentiate into pDC as well as cDC, and their preferential contribution to intestinal DC distinguishes them from other migratory DC precursors. BM pre-cDCs (lineage<sup>-</sup>B220<sup>-</sup>CD11c<sup>+</sup>MHCII<sup>-</sup> CD135<sup>+</sup>Sirpa<sup>low</sup> cells) described by Liu et al.<sup>28</sup> and splenic pre-cDC (CD11c<sup>int</sup> MHCII<sup>-</sup>CD45RA<sup>low</sup> CD43<sup>int</sup>

Sirp $\alpha^{\text{int}}$ ) described by Naik SH et al.<sup>29</sup> have a more restricted developmental potential, contributing to peripheral cDCs but not pDCs. Moreover, although pre-cDCs give rise to CD103<sup>+</sup> intestinal DCs as well as other peripheral DC populations, they lack specialized gut homing ability (they are  $\alpha 4\beta 7$  and CCR9 negative). In fact, in our co-transfer experiments, pre- $\mu$ DC are 7–10 fold better than pre-cDC at contributing to intestinal cDC on a per cell basis. Pre- $\mu$ DC are more closely related phenotypically to recently identified “CCR9<sup>-</sup>pDC-like precursors”, a common DC precursor which (like pre- $\mu$ DC and the DN DC population studied here) is B220<sup>+</sup> and expresses intermediate levels of CD11c: Schlitzer et al<sup>25,30</sup> showed elegantly that although these CCR9<sup>-</sup> pDC precursors can be induced to differentiate into cDC by GM-CSF or microenvironmental influences, they preferentially give rise to pDCs. This contrasts with the preferential cDC development displayed by pre- $\mu$ DCs. Phenotypically, CCR9<sup>-</sup> pDC precursors are defined as SiglecH<sup>hi</sup> PDCA1<sup>hi</sup> CCR9<sup>-</sup> CD11c<sup>+</sup> and B220<sup>+</sup><sup>25,30</sup>, as such they comprise a small subset of pre- $\mu$ DC (the PDCA1<sup>hi</sup>SiglecH<sup>hi</sup> fraction), as well as a large fraction of DN DCs enriched for high levels of expression of the pDC differentiation antigens PDCA1 and SiglecH. We have shown that, in contrast to pre- $\mu$ DC but similar to Schlitzer’s pDC precursors, CCR9<sup>-</sup> $\alpha 4\beta 7$ <sup>-</sup> DN DCs preferentially give rise to pDCs at early time points. We propose therefore that the Lin<sup>-</sup>B220<sup>+</sup>CD11c<sup>int</sup> CCR9<sup>-</sup> population of bone marrow cells comprises a diverse precursor pool for peripheral DC subsets, in which functional precursors with a preference towards pDC development are enriched in the PDCA1<sup>hi</sup> SiglecH<sup>hi</sup> $\alpha 4\beta 7$ <sup>-</sup> CCR9<sup>-</sup> pDC-like subset; whereas precursors biased towards development into intestinal CD103<sup>+</sup> DCs are enriched in the gut homing  $\alpha 4\beta 7^{\text{hi}}$  pre- $\mu$ DC population. Indeed, pre- $\mu$ DC themselves may well be heterogeneous in potential: we cannot exclude the possibility that some pre- $\mu$ DC are clonally committed to pDC vs. cDC development, or indeed that B220<sup>+</sup>CD11c<sup>int</sup> BM DC, including gut tropic pre- $\mu$ DC, are composed of distinct subsets of committed pDC vs. cDC precursors. This pool of B220<sup>+</sup> DC precursors was not recognized in earlier studies that included B220 as a marker of exclusion in a “lineage negative” sort gate<sup>28</sup>. In the BM, pre- $\mu$ DCs are a minor subset of this pool, which may reflect programming for rapid exit from the marrow to seed the gut wall. In addition to these CD11c<sup>+</sup> migratory precursors, earlier progenitors, including CD11c<sup>-</sup> CDPs and even pluripotent hematopoietic stem cells, may be able to seed peripheral tissues and contribute to tissue DC populations<sup>31,32</sup>. The rates of generation and exit of each of these distinctive DC precursors, their relative contributions to CD103<sup>+</sup>CD11b<sup>-</sup> vs. CD103<sup>+</sup>CD11b<sup>+</sup> intestinal DC and to other peripheral DC populations, and their relative importance in homeostatic vs. inflammatory settings remain to be determined.

The recruitment of blood leukocytes requires adhesion and chemoattractant receptors to mediate endothelial adhesion, arrest, and subsequent diapedesis<sup>33</sup>. Pre- $\mu$ DCs express  $\alpha 4\beta 7$ , an integrin receptor for the mucosal vascular addressin MAdCAM1, on gut postcapillary venules, and blockade of  $\alpha 4\beta 7$  prevents pre- $\mu$ DCs from contributing to intestinal DC populations. It is unclear which chemoattractant receptors are involved in this process. CCR9 is an important chemokine receptor for T and B lymphocytes and in CCR9<sup>+</sup> pDC homing to the SI. However, pre- $\mu$ DCs do not express CCR9. Moreover blocking antibody to the CCR9 ligand CCL25 had no effect on pre- $\mu$ DC-derived cDC in the SI, and pre- $\mu$ DCs from CCR9-knockout mice homed to and gave rise to CD103<sup>+</sup> cDCs in the SI as efficiently as wild-type cells (data not shown). Although BM pre- $\mu$ DCs express minimal CCR6, CCR6

is upregulated on pre- $\mu$ DC in the SI LP, thus CCR6 might contribute to pre- $\mu$ DC homing. Pre- $\mu$ DCs also express CCR5 and CXCR3 that could participate in gut homing. On the other hand, pre- $\mu$ DC lack the lymphoid organ trafficking receptor CCR7, consistent with their inability to home well to mesenteric lymph nodes in spite of  $\alpha 4\beta 7$  expression.

In conclusion, we identify a gut homing common DC precursor whose development in BM is regulated by retinoic acid and impaired in vitamin A deficiency. Pre- $\mu$ DCs can generate cDC and CCR9+ pDC, but more efficiently give rise to CD103+ cDC populations in the small intestines. Gut-specific homing of DC precursors may allow targeted replacement of intestinal dendritic cells as a function of ongoing tissue-specific immune requirements.

## MATERIALS AND METHODS

### Mice

C57Bl/6.CD45.2 (B6.CD45.2) and C57Bl/6.CD45.1 (B6.CD45.1) mice were originally purchased from Jackson Laboratory and were maintained and bred in specific pathogen-free conditions in the animal facility in Veterans Affairs Palo Alto Health Care Systems (VAPAHCS). To generate B16/Flt3L-injected mice, 5 million B16/Flt3L cells were injected subcutaneously near the neck and animals were sacrificed 11–14 days later. All animals were used in accordance with guidelines set forth by the animal committee of VAPAHCS. Vitamin A deficient and control mice were generated as described<sup>11</sup>. In some experiment, mice were i.p. injected with BMS493 (25mM in DMSO) at 1 $\mu$ l per gram of weight in 25  $\mu$ l of olive oil. Control animals received the same amount of DMSO in olive oil. All trans-retinoic acid was made into suspension in olive oil at 25mg/ml and injected i.p. at 125 $\mu$ g per gram of weight, control animals received olive oil. AM580 was dissolved in DMSO at a concentration of 40mg/ml and injected i.p. at 1 $\mu$ l per gram of weight with 100ml of olive oil; control animals received the same amount of DMSO in olive oil.

### Flow cytometry

Samples (single-cell suspensions) were first blocked with FACS buffer (HBSS with 2% FCS) containing 100X dilution of antibody against mouse Fc $\gamma$ III/II receptor (BD Bioscience) and rat serum to prevent non-specific binding of monoclonal antibodies. The following antibodies were used for staining: CD3-PECy7/CD3-Biotin/CD3-PerCpCy5.5 (145-2C11), CD19-PECy7/CD19-biotin/CD19-PerCpCy5.5 (ID3), NK1.1-PECy7/NK1.1-biotin/NK1.1-PerCpCy5.5 (PK136), CD49b-Biotin(DX-5), Ly6G-Biotin (1A8), Ter-119(Ter-119), B220-PECy7/B220-Biotin/B220-PerCpCy5.5 (RA3-6B2), MHCII-AF700(M5/114.15.2)/MHCII-Biotin (2G9), CD11c-PB (N418), $\alpha 4\beta 7$ -APC/ $\alpha 4\beta 7$ -PE (DATK32), CCR9-APC/CCR9-PE/CCR9-FITC (242503), CCR9-PECy7 (CW1.1), CD103-PE(M290), CD11b-AF700 (M1/70), CD8 $\alpha$ -PE (53-6.7), CD45.1-PerCpCy5.5/CD45.1-APC, CD45.2-FITC/CD45.2-PerCpCy5.5 (RA3-6B2), CD135-PE/CD135-PECy5 (A2F10), CD115-APC/CD115-FITC (AFS98), CD117-PECy7 (2B8), PDCA1-FITC/PDCA1-PerCP-eFluor710(927), SiglecH-FITC (eBio440C), Ly6C-FITC(AL-21), CD4-AF700(RM4-5), CD9-AF647 (MZ3), Sirpa-FITC/Sirpa-PerCP-eFluor710 (P84),  $\alpha 4$ -PE (9C10, BD),  $\beta 1$ -PECy7 (HMb1-1, eBioscience),  $\alpha V$ -PE (RMV-7, BD Bioscience),  $\beta 3$ -PE(2C9.G2, BD Bioscience), CD62L-FITC (MEL14), CXCR3-APC (CXCR3-173, Biolegend), CCR2-APC

(475301, R&D), CCR5-PE (2D7/CCR5, BD Bioscience), CCR7-APC(4B12, eBioscience), CXCR5-PE (BD, 2G8) and CCR6-PE (140706, R&D).

### Cell isolation from tissues

Femurs and tibias were collected and crushed using a 5ml syringe. Bone fragments were removed by filtering through a wire mesh to isolate bone marrow cells.

Spleens, inguinal, auxiliary and brachial lymph nodes (LNs) were isolated and digested with RPMI media containing 5% FCS, 500 unit/ml of collagenase IV (Worthington Biochemical) and 1 unit/ml of DNaseI (Sigma) for 30 minutes at 37°C and made into single cell suspension.

Lungs were perfused with 25 ml of PBS and cut into small pieces (~1–2mm) and digested as were spleen and LNs.

Full-length SI (with Peyer's Patches removed) was cut open longitudinally and rinsed twice in HBSS (without Ca<sup>2+</sup> and Mg<sup>2+</sup>) with 2% FCS and cut into small pieces. To isolate IEL, the cut SI was incubated twice in 10 ml of 2% HBSS containing 15 mg/100ml dithiothreitol (DTT) at 37 °C for 20 minute, twice, and supernatant containing IEL was collected after each incubation. Residual tissues were digested in 10 ml RPMI containing 5% FCS and 0.5 mg/ml of collagenase IV (Sigma C2139) at 37°C for 30 minutes, three times. Supernatant containing LP cells was collected. Mononucleated cells from the IEL and LP supernatant were isolated by gradient separation with 40% and 75% percoll solutions (GE, 17-0891-01) at 2000 RPMI for 20 minutes at room temperature. Cells of interest were located at the interface. When young mice (10–16 days of age) were used, Peyer's Patches were not removed because they are not clearly visible at this age.

### Cell sorting

To sort pre- $\mu$ DCs and DN DCs from normal and Flt3L-treated mice, BM cells were isolated as described above and enriched by magnetic activated cell sorting (MACS) using the pan-DC kits from Miltenyi. The cells were then sorted on Aria II or III (BD) for Lineage (CD3, CD19, NK1.1)-CD11c<sup>int</sup>B220<sup>+</sup> $\alpha$ 4 $\beta$ 7<sup>+</sup>CCR9<sup>-</sup> pre- $\mu$ DC and Lineage<sup>-</sup> CD11c<sup>int</sup>B220<sup>+</sup> $\alpha$ 4 $\beta$ 7<sup>-</sup>CCR9<sup>-</sup> DN DC.

### Adoptive transfer

For transfer into lethally irradiated recipients, B6.CD45.1/45.2 F1 mice were given full body irradiation with a lethal dose of 900 rads total from a 131 Cs source at two doses (4 hours apart, 450 rads each). Irradiated mice were given total BM (CD45.1) and sorted pre- $\mu$ DCs (CD45.2 or vice versa) at a ratio of 10:1 ( $5 \times 10^6$  total BM and  $0.5 \times 10^6$  sorted pre- $\mu$ DC). Mice were kept on antibiotic water until they were sacrificed on day 4, 7, 10 or 14. Adoptive transfer into normal recipients was performed the same way except recipient mice were not irradiated and received only sorted pre- $\mu$ DC ( $1-3 \times 10^6$ ). For homing experiments,  $3 \times 10^6$  sorted pre- $\mu$ DCs were transferred into each congenic recipient.

## Blocking experiments

Sorted pre- $\mu$ DC from Flt3L-treated mice were pre-blocked with 250  $\mu$ g of anti- $\alpha$ 4 $\beta$ 7 antibody made in house (DATK32) or isotype control (Rat IgG2a) in 200 ml PBS for 10 minute at room temperature before injection. Subsequently recipients received blocking antibody or isotype control every 12 hours via intraperitoneal injection until mice were sacrificed. All cell transfers were done via retro-orbital injection.

## *In vitro* culture

Pre- $\mu$ DCs and DN DCs were sorted from BM (or SI LP for pre- $\mu$ DC in some experiments) from normal or Flt3L-treated mice and cultured with congenic total BM cells at a density of 3–5 million cells/ml, 200 $\mu$ l per well in flat-bottom 96-well plate in complete RPMI media (10% FCS, 1X penicillin/streptomycin) supplemented with 100ng/ml recombinant Flt3L. Media were changed on day 3. Total BM cells were cultured in complete media with normal FCS or delipidated FCS with 100ng/ml of rFlt3L in the presence of 1nM of ATRA, 10nM of AM580 or 100nM of BMS493. Media were changed on day 3.

CFSE labeling: Total BM cells were incubated with 1 $\mu$ M of CFSE at a density of 10E6 cells/ml in PBS for 10 min at 37°C and washed by incubating in complete media for 5 min at 37°C.

## Analysis of ALDH activity

Aldehyde dehydrogenase (ALDH) activity in each cell was analyzed using Aldefluor Staining Kit (StemCell Technologies) per the manufacturer's protocol with modifications as previously described<sup>18</sup>. Briefly, cells were suspended in Aldefluor assay buffer containing activated substrate (150 nM) with or without the ALDH inhibitor DEAB (100 $\mu$ M) at a density of 10E6 cells/ml and incubated in 37°C water bath for 30 minutes. Subsequent surface antigen staining was performed in Aldefluor assay buffer. Cells were immediately analyzed on LSRII analyzer (BD) without fixing.

## Statistical Analysis

The statistical significance of differences between two sets of data was assessed by Student's t-test unless stated otherwise.

## Supplementary Material

Refer to Web version on PubMed Central for supplementary material.

## Acknowledgments

We thank L. Rott for assistance with flow cytometry and cell sorting and WW Agace for critical comments on early studies. The B16 melanoma cell line stably transfected with murine Flt3L was a kind gift from G. Dranoff, Dana-Farber Cancer Institute, Boston, MA. R.Z. is a recipient of the National Science Scholarship awarded by the Agency for Science, Technology And Research, Singapore; C.O. was supported by the Wenner-Gren Foundation, and by a Research Fellowship Award (#2791) from the Crohn's & Colitis Foundation of America; R.Y. is supported by the Immunology training grant (5 T32 AI07290, Molecular and Cellular Immunobiology); M.L. is a recipient of a senior fellowship from the Crohn's and Colitis Foundation, and was a fellow under the NIH Training Grant AI07290; H.H. is a recipient of an Investigator Career Award from the Arthritis Foundation and was a fellow under the NIH Training Grant AI07290; A.H. was supported by NIH grant DK085426. The work was supported in

part by NIH grants AI047822, AI093981 and DK084647 to E.C.B., the FACS Core facility of the Stanford Digestive Disease Center under DK056339, and a Merit Award from the Department of Veterans Affairs.

## References

1. Annacker O, Coombes JL, Malmstrom V, et al. Essential role for CD103 in the T cell-mediated regulation of experimental colitis. *J Exp Med.* Oct 17; 2005 202(8):1051–1061. [PubMed: 16216886]
2. Bogunovic M, Ginhoux F, Helft J, et al. Origin of the lamina propria dendritic cell network. *Immunity.* Sep 18; 2009 31(3):513–525. [PubMed: 19733489]
3. Iwasaki A. Mucosal dendritic cells. *Annu Rev Immunol.* 2007; 25:381–418. [PubMed: 17378762]
4. Johansson-Lindbom B, Svensson M, Pabst O, et al. Functional specialization of gut CD103+ dendritic cells in the regulation of tissue-selective T cell homing. *J Exp Med.* Oct 17; 2005 202(8): 1063–1073. [PubMed: 16216890]
5. Silva MA. Intestinal dendritic cells and epithelial barrier dysfunction in Crohn's disease. *Inflamm Bowel Dis.* Mar; 2009 15(3):436–453. [PubMed: 18821596]
6. Salazar-Gonzalez RM, Niess JH, Zammit DJ, et al. CCR6-mediated dendritic cell activation of pathogen-specific T cells in Peyer's patches. *Immunity.* May; 2006 24(5):623–632. [PubMed: 16713979]
7. Varol C, Vallon-Eberhard A, Elinav E, et al. Intestinal lamina propria dendritic cell subsets have different origin and functions. *Immunity.* Sep 18; 2009 31(3):502–512. [PubMed: 19733097]
8. Coombes JL, Siddiqui KR, Arancibia-Carcamo CV, et al. A functionally specialized population of mucosal CD103+ DCs induces Foxp3+ regulatory T cells via a TGF-beta and retinoic acid-dependent mechanism. *J Exp Med.* Aug 6; 2007 204(8):1757–1764. [PubMed: 17620361]
9. Geissmann F, Manz MG, Jung S, Sieweke MH, Merad M, Ley K. Development of monocytes, macrophages, and dendritic cells. *Science.* Feb 5; 327(5966):656–661. [PubMed: 20133564]
10. Jaensson-Gyllenback E, Kotarsky K, Zapata F, et al. Bile retinoids imprint intestinal CD103+ dendritic cells with the ability to generate gut-tropic T cells. *Mucosal immunology.* Jul; 2011 4(4): 438–447. [PubMed: 21289617]
11. Iwata M, Hirakiyama A, Eshima Y, Kagechika H, Kato C, Song SY. Retinoic acid imprints gut-homing specificity on T cells. *Immunity.* Oct; 2004 21(4):527–538. [PubMed: 15485630]
12. Hill JA, Hall JA, Sun CM, et al. Retinoic acid enhances Foxp3 induction indirectly by relieving inhibition from CD4+CD44hi Cells. *Immunity.* Nov 14; 2008 29(5):758–770. [PubMed: 19006694]
13. Berlin C, Berg EL, Briskin MJ, et al. Alpha 4 beta 7 integrin mediates lymphocyte binding to the mucosal vascular addressin MAdCAM-1. *Cell.* Jul 16; 1993 74(1):185–195. [PubMed: 7687523]
14. Mach N, Gillessen S, Wilson SB, Sheehan C, Mihm M, Dranoff G. Differences in dendritic cells stimulated in vivo by tumors engineered to secrete granulocyte-macrophage colony-stimulating factor or Flt3-ligand. *Cancer Res.* Jun 15; 2000 60(12):3239–3246. [PubMed: 10866317]
15. Edelson BT, Kc W, Juang R, et al. Peripheral CD103+ dendritic cells form a unified subset developmentally related to CD8alpha+ conventional dendritic cells. *The Journal of experimental medicine.* Apr 12; 2010 207(4):823–836. [PubMed: 20351058]
16. Agace WW, Persson EK. How vitamin A metabolizing dendritic cells are generated in the gut mucosa. *Trends in immunology.* Jan; 2012 33(1):42–48. [PubMed: 22079120]
17. Schulz O, Jaensson E, Persson EK, et al. Intestinal CD103+, but not CX3CR1+, antigen sampling cells migrate in lymph and serve classical dendritic cell functions. *J Exp Med.* Dec 21; 2009 206(13):3101–3114. [PubMed: 20008524]
18. Yokota A, Takeuchi H, Maeda N, et al. GM-CSF and IL-4 synergistically trigger dendritic cells to acquire retinoic acid-producing capacity. *International immunology.* Apr; 2009 21(4):361–377. [PubMed: 19190084]
19. Chute JP, Ross JR, McDonnell DP. Minireview: Nuclear receptors, hematopoiesis, and stem cells. *Mol Endocrinol.* Jan; 2010 24(1):1–10. [PubMed: 19934345]

20. Safi R, Muramoto GG, Salter AB, et al. Pharmacological manipulation of the RAR/RXR signaling pathway maintains the repopulating capacity of hematopoietic stem cells in culture. *Mol Endocrinol.* Feb; 2009 23(2):188–201. [PubMed: 19106195]
21. Chute JP, Muramoto GG, Whitesides J, et al. Inhibition of aldehyde dehydrogenase and retinoid signaling induces the expansion of human hematopoietic stem cells. *Proceedings of the National Academy of Sciences of the United States of America.* Aug 1; 2006 103(31):11707–11712. [PubMed: 16857736]
22. Kastner P, Chan S. Function of RARalpha during the maturation of neutrophils. *Oncogene.* Oct 29; 2001 20(49):7178–7185. [PubMed: 11704846]
23. Hess DA, Meyerrose TE, Wirthlin L, et al. Functional characterization of highly purified human hematopoietic repopulating cells isolated according to aldehyde dehydrogenase activity. *Blood.* Sep 15; 2004 104(6):1648–1655. [PubMed: 15178579]
24. Segura E, Wong J, Villadangos JA. Cutting edge: B220+CCR9-dendritic cells are not plasmacytoid dendritic cells but are precursors of conventional dendritic cells. *J Immunol.* Aug 1; 2009 183(3):1514–1517. [PubMed: 19570827]
25. Schlitzer A, Loschko J, Mair K, et al. Identification of CCR9-murine plasmacytoid DC precursors with plasticity to differentiate into conventional DCs. *Blood.* Jun 16; 2011 117(24):6562–6570. [PubMed: 21508410]
26. Watowich SS, Liu YJ. Mechanisms regulating dendritic cell specification and development. *Immunological reviews.* Nov; 2010 238(1):76–92. [PubMed: 20969586]
27. Franco CB, Chen CC, Drukker M, Weissman IL, Galli SJ. Distinguishing mast cell and granulocyte differentiation at the single-cell level. *Cell Stem Cell.* Apr 2; 2010 6(4):361–368. [PubMed: 20362540]
28. Liu K, Victora GD, Schwickert TA, et al. In vivo analysis of dendritic cell development and homeostasis. *Science.* Apr 17; 2009 324(5925):392–397. [PubMed: 19286519]
29. Naik SH, Metcalf D, van Nieuwenhuijze A, et al. Intrasplenic steady-state dendritic cell precursors that are distinct from monocytes. *Nature immunology.* Jun; 2006 7(6):663–671. [PubMed: 16680143]
30. Schlitzer A, Heiseke AF, Einwachter H, et al. Tissue-specific differentiation of a circulating CCR9-pDC-like common dendritic cell precursor. *Blood.* Jun 21; 2012 119(25):6063–6071. [PubMed: 22547585]
31. Schmid MA, Takizawa H, Baumjohann DR, Saito Y, Manz MG. Bone marrow dendritic cell progenitors in mice sense pathogens via Toll-like receptors and subsequently migrate to inflamed lymph nodes. *Blood.* Sep 9.2011
32. Massberg S, Schaerli P, Knezevic-Maramica I, et al. Immunosurveillance by hematopoietic progenitor cells trafficking through blood, lymph, and peripheral tissues. *Cell.* Nov 30; 2007 131(5):994–1008. [PubMed: 18045540]
33. Butcher EC. Leukocyte-endothelial cell recognition: three (or more) steps to specificity and diversity. *Cell.* Dec 20; 1991 67(6):1033–1036. [PubMed: 1760836]

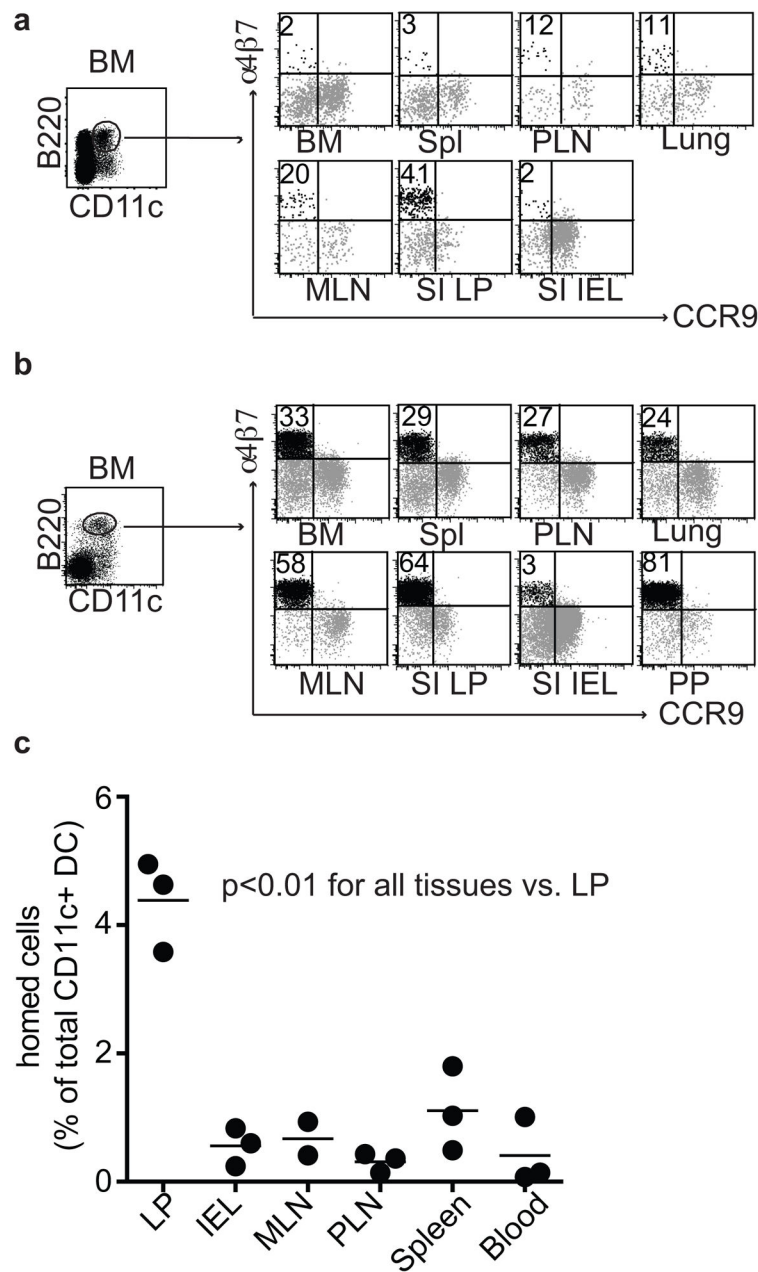


**Figure 1. Identification of a phenotypically unique  $\alpha 4\beta 7$  expressing, gut-homing DC subset *in vivo*.**

a) Surface expression of  $\alpha 4\beta 7$  and CCR9 on live  $\text{lin}^- \text{CD11c}^+ \text{B220}^+$  DCs from lymphoid and non-lymphoid tissues from 2–3 week old C57Bl/6 mice;  $\text{lin}$  indicates CD3, CD19, and NK1.1. Data are representative of seven independent experiments. b) Surface expression of  $\alpha 4\beta 7$  and CCR9 on live  $\text{lin}^- \text{CD11c}^+ \text{B220}^+$  DCs from lymphoid and non-lymphoid tissues taken from Flt3L-treated mice. Data are representative of at least three independent experiments. c) Three million purified pre- $\mu$ DCs, sorted from peripheral lymphoid tissues from Flt3L-treated B6.CD45.2 mice, were transferred intravenously into B6.CD45.1 recipients. Tissues were harvested on day 3 after transfer and donor-derived cells were

quantified. Data are presented as the percentage of total CD11c<sup>+</sup> host cells. Each dot represents 1 individual animal, n=3 from two independent experiments. p<0.01 for LP vs. all other tissues by Student's *t*-test.

Author Manuscript

Author Manuscript

Author Manuscript

Author Manuscript

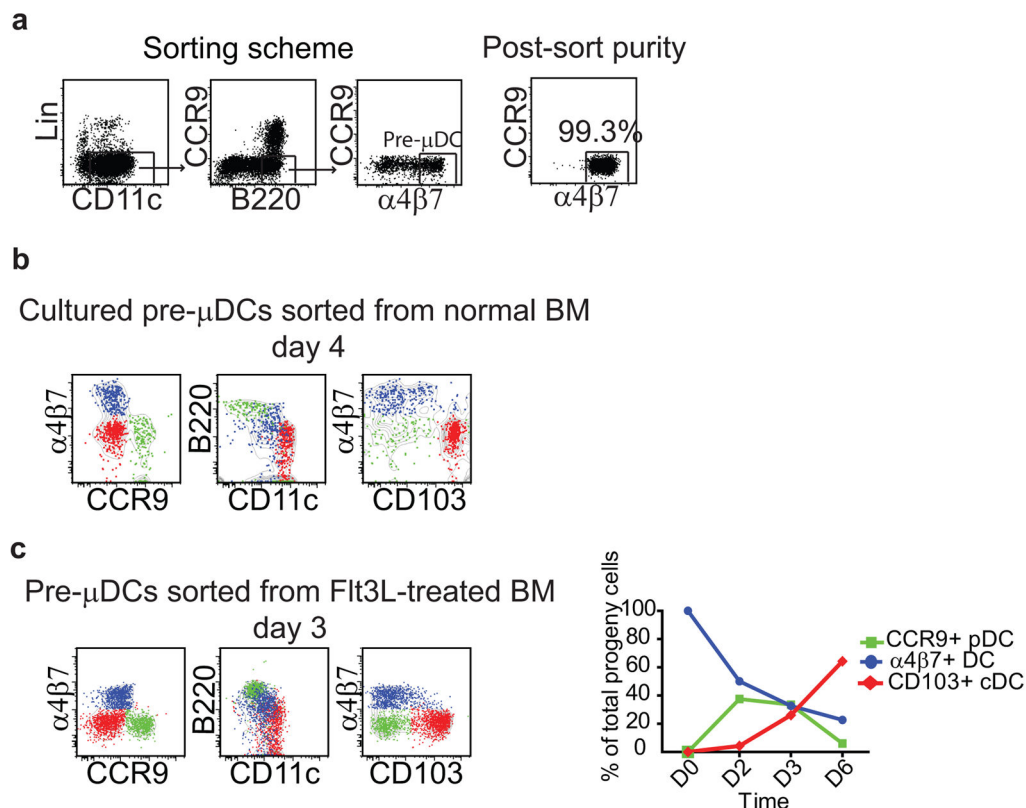
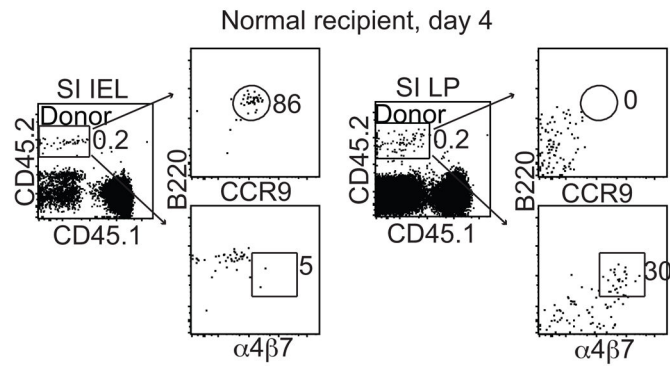


**Figure 2. Pre- $\mu$ DCs give rise to CCR9<sup>+</sup> pDCs and to CD103<sup>+</sup> cDCs *in vitro***

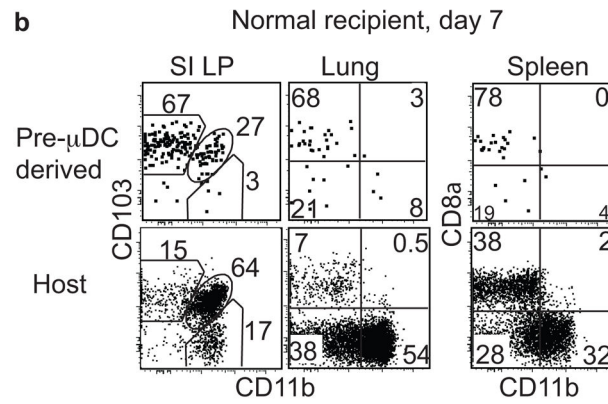
a) Sorting scheme and purity analysis for pre- $\mu$ DCs. Lin indicates CD3, CD19, and NK1.1.

b) Pre- $\mu$ DCs were sorted from BM of B6.CD45.2 mice and cultured with total BM taken from congenic B6.CD45.1 mice in complete RPMI supplemented with 100 ng/ml rFlt3L. Cultured cells were analyzed by flow cytometry on day 4. Pre- $\mu$ DC-derived cells on day 4 included three distinct populations: CCR9<sup>+</sup> DCs (green), CD103<sup>+</sup> DCs (red) and  $\alpha 4\beta 7$ <sup>+</sup> DCs (blue). Grey contour plots show all pre- $\mu$ DC-derived cells. Data represent one of three independent experiments with similar results. c) Pre- $\mu$ DCs were sorted from Flt3L-treated mouse BM and cultured in the conditions described in panel b legend. Pre- $\mu$ DC derived cells on day 3 consist of three populations similar to those from untreated mice. Line graphs show that by day 6, most pre- $\mu$ DC-derived CCR9<sup>+</sup> pDCs disappeared and the cultures consisted mostly of CD103<sup>+</sup> cDCs. Data are representative of three independent experiments with similar results.

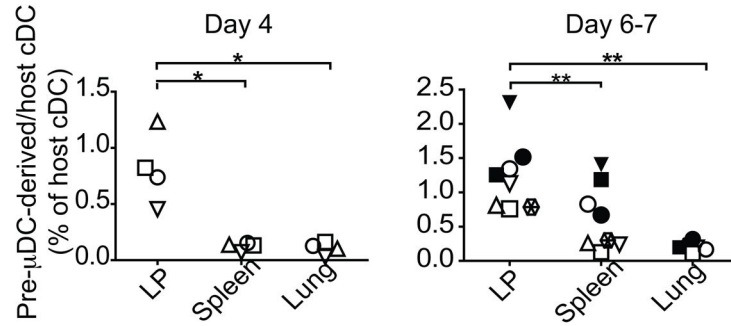
a

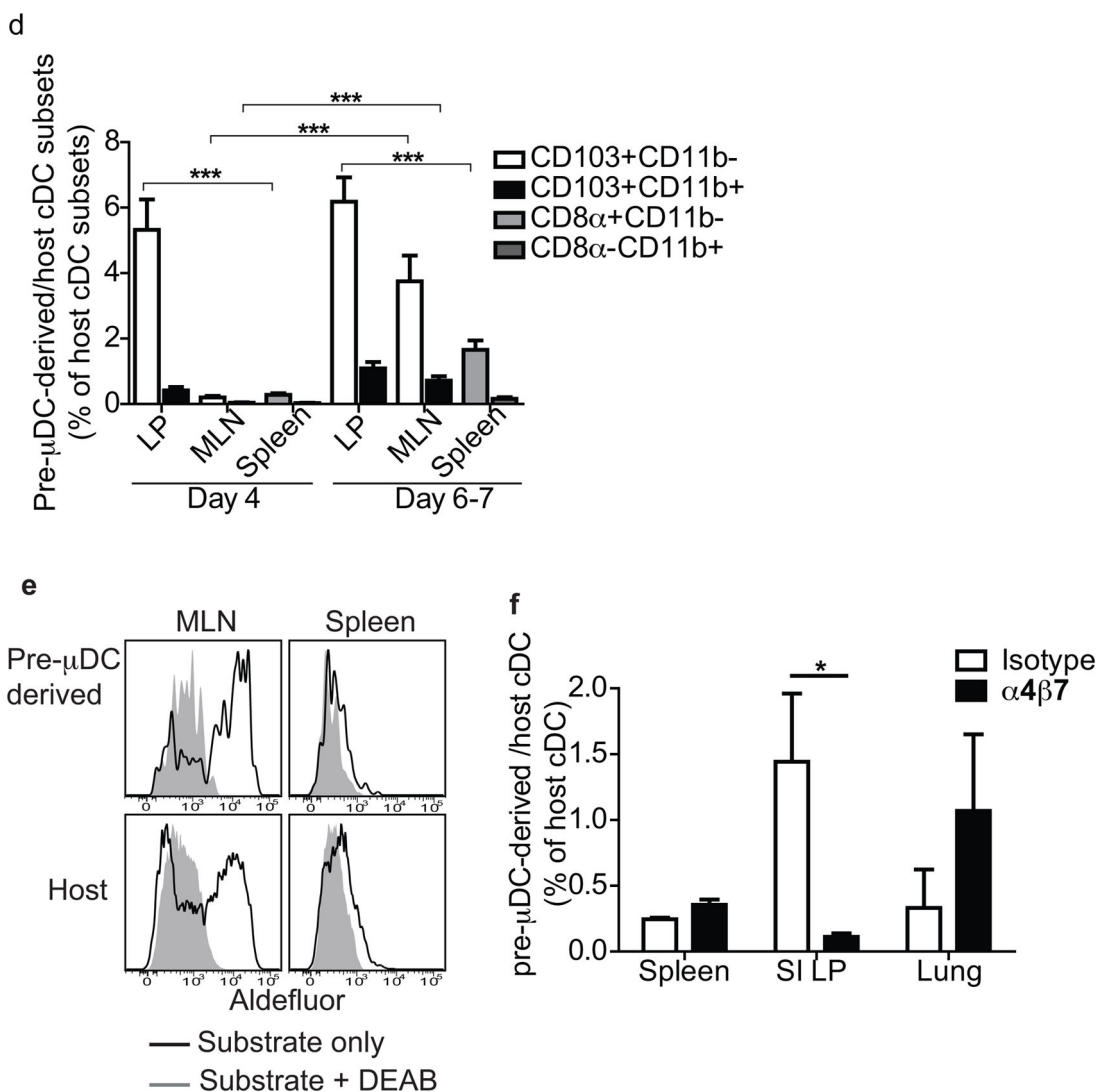


b



c

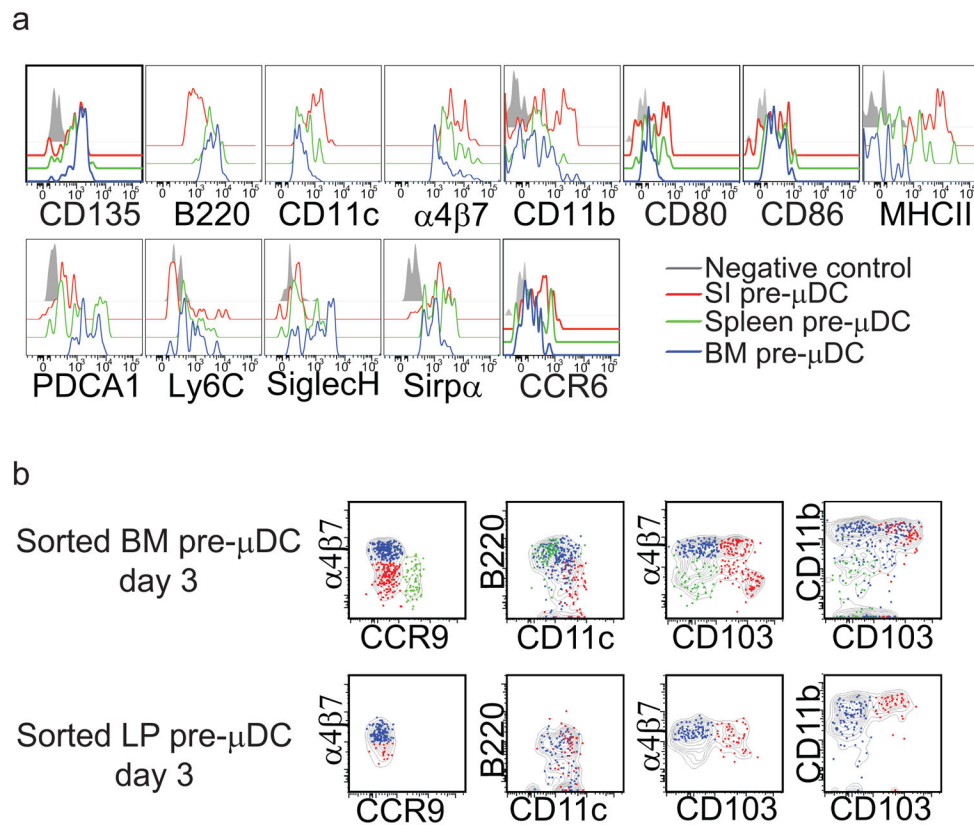




**Figure 3. Pre-μDCs give rise to CD103<sup>+</sup> cDCs and to CCR9<sup>+</sup> pDC *in vivo* and preferentially reconstitute the small intestine**

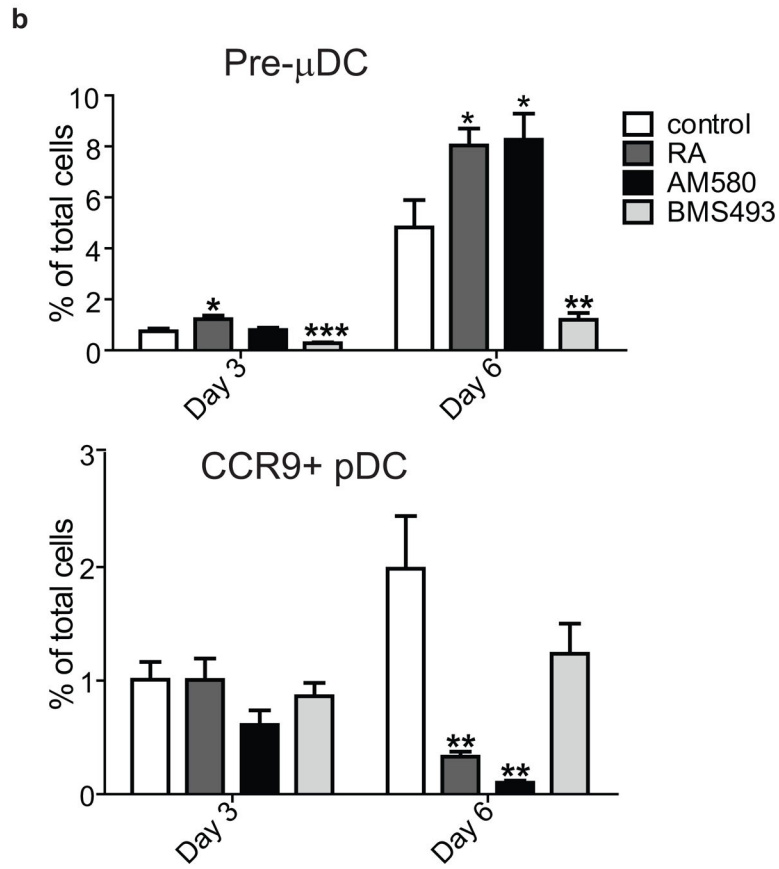
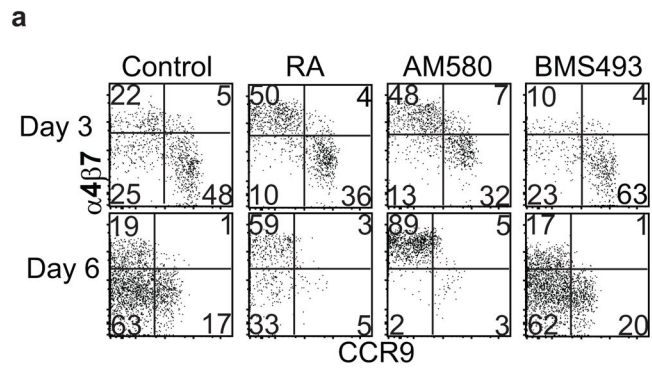
One to 2.5 million FACS-sorted pre-μDCs (CD45.2) were injected into CD45.1 recipients and analyzed on day 4 and day 6 or 7. Day 4: n=4 from two independent experiments. Day 6 or 7: n=8 from five independent experiments. \* p<0.05, \*\* p<0.01, \*\*\* p<0.001 by Student's *t*-test. a) CCR9, α4β7 and B220 expression on total pre-μDC-derived cells (CD45.2) in SI IEL (left) and LP (right) on day 4 after transfer. Numbers indicate percentage cells. Data shown are from one of four recipients with similar results. b) CD103 and CD11b on pre-μDC-derived CD11c<sup>+</sup> cells and host CD11c<sup>+</sup> cells on day 7. The plot shows data from one of eight recipients with similar results. c) Pre-μDC-derived CD11c<sup>+</sup> cells (per million input cells) as percentage of host CD11c<sup>+</sup> cells in different tissues on day 4 and day 6 or 7. Symbols of the same shape and color represent tissues from the same animal. d) Pre-μDC-derived CD103<sup>+</sup>CD11b<sup>-</sup> and CD103<sup>+</sup>CD11b<sup>+</sup> cDCs from SI LP or MLN and CD8α<sup>+</sup>CD11b<sup>-</sup> and CD8α<sup>-</sup>CD11b<sup>+</sup> cDCs from spleen are shown as percentage of the corresponding subset from the host on day 4 and day 6 or 7 after transfer. e) Aldefluor

staining of pre- $\mu$ DC-derived and host CD11c<sup>+</sup> cDCs from MLN and spleen. Negative control staining in the presence of ALDH inhibitor DEAB is shown for comparison. Data are representative of three independent experiments with similar results. f) Pre- $\mu$ DCs were sorted from Flt3L-treated mice and pre-incubated with 250  $\mu$ g of either  $\alpha$ 4 $\beta$ 7-blocking antibody (DATK32) or isotype control for 10 minutes at room temperature before transfer into congenic recipients. Recipient mice received 250  $\mu$ g of  $\alpha$ 4 $\beta$ 7-blocking antibody or isotype control every 12 hours and were sacrificed on day 4. Pre- $\mu$ DC-derived total CD11c<sup>+</sup> cells were calculated as percentage of host CD11c<sup>+</sup> cells. Data show combined results from analyses of three mice from two independent experiments. Error bars show SEM. \*  $p < 0.05$  by Student's *t*-test.



**Figure 4. SI pre- $\mu$ DCs are more differentiated than BM pre- $\mu$ DCs and have lost potential to give rise to CCR9<sup>+</sup> pDCs**

a) Surface antigen expression on pre- $\mu$ DCs from the BM, spleen, and SI LP. b) pre- $\mu$ DCs were FACS sorted from BM and SI LP and cultured with congenic total BM feeder cells in complete RPMI supplemented with 100 ng/ml rFlt3L. Cultures were analyzed by flow cytometry on day 3. Pre- $\mu$ DC-derived subsets are coded as follows: green, CCR9<sup>+</sup>; blue,  $\alpha 4\beta 7$ <sup>+</sup>; red, CD103<sup>+</sup>; grey contour plot indicates total pre- $\mu$ DC-derived cells. Data are representative of two experiments with similar results.



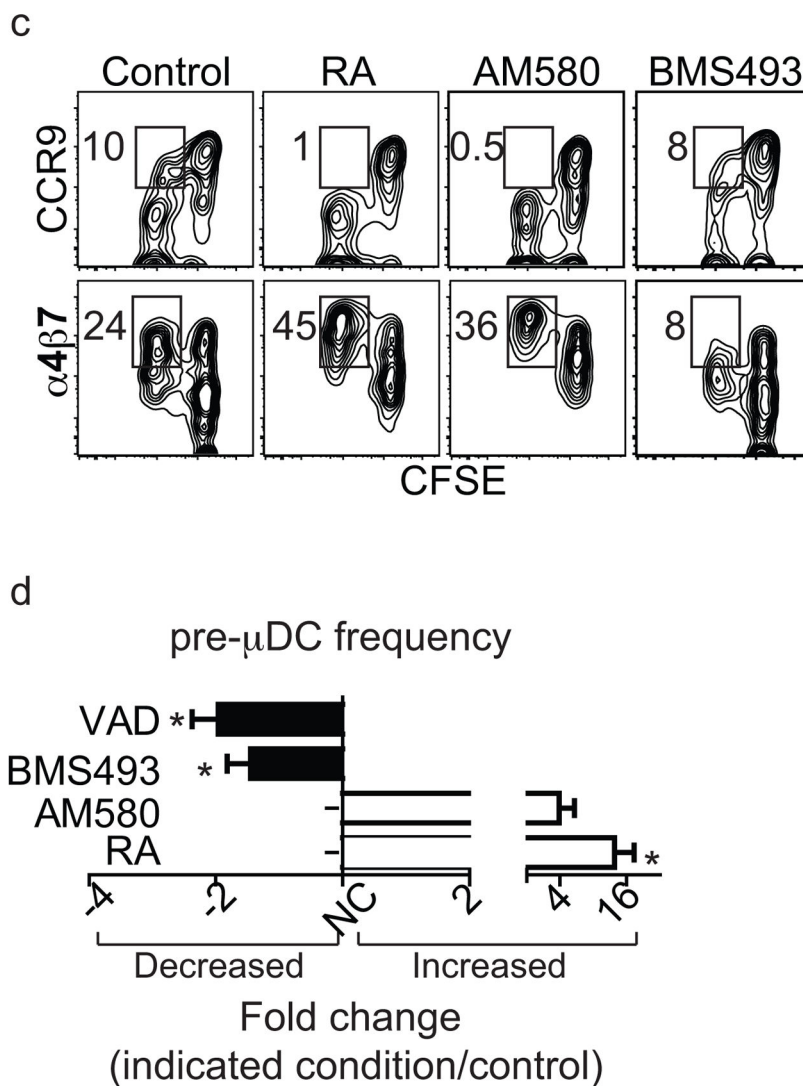


### Figure 5. Retinoic acid regulates pre- $\mu$ DC development in the BM

a–b) Total BM cells were cultured in complete media supplemented with 100 ng/ml of Flt3L in the absence (control) or presence of 1 nM RA, 10 nM AM580 (an RAR $\alpha$  agonist), or 100 nM BMS498 (a pan RAR inverse agonist). Cells were harvested on days 3 and 6 and stained for pre- $\mu$ DC and CCR9<sup>+</sup> pDC markers. a) Cells were gated on Lin<sup>-</sup>CD11c<sup>+</sup>B220<sup>+</sup> (Lin indicates CD3, CD19, DX-5, Ter-119, Ly6G). Numbers in each quadrant indicate percent cells. b) Percent of pre- $\mu$ DCs (top) and CCR9<sup>+</sup> pDCs (bottom) on days 3 and 6 in total BM cultures, grown under the conditions described in panel a legend. Data show combined results from four independent experiments with n=6–8 for each condition. Error bars show SEM. \* p<0.05, \*\*p<0.01, \*\*\*p<0.001 compared to control by Student's *t*-test. c) Total BM cells were labeled with CFSE and cultured as described in the panel a legend. Cultures were harvested on day 3 and cells were gated on Lin<sup>-</sup>CD11c<sup>+</sup>B220<sup>+</sup>. Numbers indicate percentage cells. d) Fold change of pre- $\mu$ DC frequency in BM from mice treated with each indicated condition compared to control. VAD: vitamin A deficient mice, n=10, control: n=8; BMS493/AM580/RA: mice received BMS493 or vehicle (for 7–18 days, n=4 each),

AM580 or vehicle (4–6 days, n=2) or RA or vehicle (4–6 days, n=3). Pre- $\mu$ DC frequency (among total BM cells) was determined. The fold change in frequency in treated vs. control mice in each paired comparison was calculated, and is shown with SEM or (for AM580) range. \*  $p < 0.05$  by Mann Whitney test between treated and control mice.

Author Manuscript

Author Manuscript

Author Manuscript

Author Manuscript